

Article

# A Novel Simplified Algorithm for Bare Surface Soil Moisture Retrieval Using L-Band Radiometer

Bin Zhu <sup>1</sup>, Xiaoning Song <sup>1,\*</sup>, Pei Leng <sup>2</sup>, Chuan Sun <sup>1</sup>, Ruixin Wang <sup>1</sup> and Xiaoguang Jiang <sup>1</sup>

<sup>1</sup> University of Chinese Academy of Sciences, Beijing 100049, China; zhubin14@mailsucas.ac.cn (B.Z.); sunchuan14@mailsucas.ac.cn (C.S.); wangruixin14@mailsucas.ac.cn (R.W.); xgjiang@ucas.ac.cn (X.J.)

<sup>2</sup> Key Laboratory of Agri-Informatics, Ministry of Agriculture/Institute of Agricultural Resources and Regional Planning, Chinese Academy of Agricultural Sciences, Beijing 100081, China; lengpei@caas.cn

\* Correspondence: songxn@ucas.ac.cn; Tel.: +86-10-8825-6376

Academic Editors: Zhao-Liang Li, Jose A. Sobrino, Chao Ren and Wolfgang Kainz

Received: 25 May 2016; Accepted: 4 August 2016; Published: 9 August 2016

**Abstract:** Soil moisture plays an important role in understanding climate change and hydrology, and L-band passive microwave radiometers have been verified as effective tools for monitoring soil moisture. This paper proposes a novel, simplified algorithm for bare surface soil moisture retrieval using L-band radiometer. The algorithm consists of two sub-algorithms: a surface emission model and a soil moisture retrieval model. In analyses of the advanced integral equation model (AIEM) simulated database, the surface emission model was developed to diminish the effects of surface roughness using dual-polarization surface reflectivity. The soil moisture retrieval model, which was calibrated using the Dobson simulated database, is based on the relationship between the adjusted real refractive index  $N_r$  and the volumetric soil moisture. Soil moisture can be determined via a numerical solution that uses several freely available input parameters: dual-polarization microwave brightness temperature, surface temperature, and the contents of sand and clay. The results showed good agreement with the input soil moisture values simulated by the AIEM model, with root mean square errors (RMSEs) lower than 3% at all incidence angles. The algorithm was then verified based on data from the four-year L-band experiments conducted at Beltsville Agricultural Research Center (BARC) test sites, achieving RMSEs of 4.3% and 3.4% at 40° and 50°, respectively. These results indicate that the simplified algorithm proposed in this paper shows a very good accuracy in soil moisture retrieval. Additionally, the algorithm exhibits a better performance for the large incidence angle radiometers in L-band such as those produced by the Soil Moisture Active and Passive (SMAP).

**Keywords:** L-band; advanced integral equation model (AIEM); Dobson model; surface soil moisture; surface roughness

## 1. Introduction

Soil moisture is an important parameter in the global energy balance and water cycle. In addition, it plays a crucial role in water resources management, vegetation growth, flood monitoring, and climate prediction [1–3]. Remote sensing is one of the most effective tools used in soil moisture monitoring due to its wide range of observations and the high frequency of repeated measurements. Currently, microwave remote sensing is considered an effective way to measure soil moisture because it can penetrate clouds and vegetation and works in both daytime and nighttime in all-weather conditions, particularly in L-band. L-band microwave radiometers show great potential for monitoring soil moisture because they experience little attenuation in the atmosphere, have strong vegetation penetration capability, and have high sensitivity to soil moisture. Therefore, many satellite missions use L-band radiometers for soil moisture monitoring. The Soil Moisture and Ocean Salinity (SMOS) mission uses a multi-angle L-band radiometer [1], while the Soil Moisture Active and Passive (SMAP)

and Aquarius missions both carry L-band radar and radiometers [2,4]. The scheduled Water Cycle Observation Mission (WCOM) uses a tri-frequency radiometer that includes L-band [5].

Many algorithms have been developed for L-band radiometers. The surface emission model is a crucial component of these algorithms; it mainly considers surface roughness based on surface emissivity. Because surface roughness is difficult to measure at large scales, several models have been proposed to estimate the effect of surface roughness, including both physical and semi-empirical models. Physical models such as the Integral Equation Model (IEM) and the Advanced Integral Equation Model (AIEM) [6] are highly complex and include many unmeasurable parameters. Although these models provide detailed descriptions of radiative processes, their complexities restrict their applications. In contrast, semi-empirical models utilize simplified parameters that can be retrieved easily. Almost all of the algorithms associated with soil moisture retrieval were developed from semi-empirical models. The  $H_p$  model was proposed by Choudhury [7], who considered the non-coherent component to be relatively small at a low frequency. This model is commonly used in L-band soil moisture retrieval and has been developed into many other semi-empirical models. However, the surface roughness parameters in those models are mainly expressed as constant values according to different regions, increasing the uncertainties due to strong surface heterogeneity. Shi [8] presented a parameterized model for L-band based on the IEM simulated database; however, this model is not simple enough for practical applications. Recently, some models have been created by analyzing dual-polarization surface reflectivity using the AIEM simulated database [9–12]. These new methods utilize dual polarization to reduce the dependence on surface roughness parameters, making the algorithm more reliable. The surface emission model proposed in this study is based on these methods.

After considering the effects of surface roughness, soil moisture can be calculated using three basic methods: an inverse iteration algorithm, a forward numerical algorithm, and an empirical algorithm. The inverse iteration algorithm is commonly used in many single channel algorithms [13]. First, the soil moisture is set to an initial value according to different regions. Then, the Fresnel reflectivity is calculated inversely based on the Fresnel reflectivity equation. Finally, the simulated value is iterated based on the observed value using a least-squares algorithm until convergence. In dual-channel and multi-channel radiometers, the forward numerical algorithm is widely adopted. Soil moisture is retrieved by minimizing a cost function using a least-squares iterative algorithm [14]. This method performs well in making the best use of multi-channel data. The empirical algorithm comprises several empirical equations that describe the uncertain relationships of parameters. Given sufficient training data, this algorithm provides good accuracy in specific areas [15–18]. However, the weaknesses of these models are still quite apparent. In the inverse iteration algorithm, the phenomenon of pseudo-convergence is difficult to avoid. As for the forward numerical algorithm, the cost function is always based on several retrieved parameters (soil moisture, optical depth at nadir and the soil roughness parameter) [14]. All of these parameters have effects in minimizing the differences between the measured and simulated values. Therefore, the iterative algorithm cannot explain which parameter is responsible for changing the satellite measurement in mechanism [19]. The constraints and initial values set in the cost function also add uncertainty factors to the algorithm. In both the inverse iteration and the forward numerical algorithm, the soil dielectric model is adopted to estimate the effects of soil, which brings considerable soil ancillary data and introduces more uncertainties into the algorithm. The empirical algorithm lacks clear physical significance, making it difficult to apply at large scales. Considering the limitations of these models, a new algorithm is proposed in this paper.

The objective of this study is to develop a new algorithm that can easily be applied for L-band soil moisture retrieval. The physically based algorithm combines two sub-algorithms: a surface emission model and a soil moisture retrieval model. The surface emission model addresses the effects of surface roughness. This model is based on dual-polarization surface reflectivity with no surface roughness parameters required. The soil moisture retrieval model concentrates on the soil dielectric properties. This retrieval model utilized an analytic solution that is based on the physical model and requires only

the contents of sand and clay during the retrieval process. The main improvement of this algorithm is that it has fewer uncertain parameters and is physically based, with no regional dependence.

The rest of this paper is organized as follows. Section 2 describes the study area and the field datasets used in this study. Section 3 introduces the algorithm proposed in this study. Section 4 presents the experimental results and a sensitivity analysis of the new model. The conclusions of the paper are summarized in Section 5.

## 2. Study Area and Datasets

### 2.1. Study Area

From 1979 to 1982, the NASA/Goddard Space Flight Center (GSFC) and the United States Department of Agriculture (USDA)/Beltsville Agricultural Research Center (BARC) conducted four-year experiments at BARC test sites [20–23]. The objective of these experiments was to study the effects of soil texture, surface roughness, and vegetation cover on remote estimates of soil moisture content using microwave radiometers [21]. The study was conducted at several local agricultural test sites in Beltsville, Maryland, which contained different soil types and vegetation cover. Observations of soil moisture, soil temperature, vegetation biomass and other soil and canopy parameters were made concurrently with the microwave measurements [23]. These data have since been widely used to validate different models of soil moisture retrieval [9,10]. In this study, the bare surface test sites were chosen as the study area.

### 2.2. Microwave Data

The microwave data were acquired with L-band (1.4 GHz) radiometers mounted on a boom truck. The sensors were dual-polarized Dicke radiometers, which measure thermal microwave emission at different incidence angles ranging from 10° to 70° in 10° steps. Calibration of the microwave system was verified every day using a cold sky reflector and a microwave absorbing material (Eccosorb). The estimated accuracy of the L-band radiometer is approximately  $\pm 3$  K [23].

### 2.3. Field Data

The four-year experiment was performed at the BARC test sites. In 1979 and 1980, a field with sandy loam soil in Elinsboro was selected. Two new test sites were chosen in 1981 and 1982: one in Edmonston and the other in South Farm. In 1982, three sites were selected: the two previous sites plus a site in Gish. The field data were measured from bare surfaces and included soil bulk density, soil moisture, and soil temperature. Precise soil bulk density and texture measurements were made several times at each test site during the experiments [23]. Detailed descriptions of all the bare surface sites are listed in Table 1. Soil moisture was measured at depths of 0–0.5 cm, 0–2.5 cm, 2.5–5 cm, and 5–10 cm. Soil temperature profiles were sampled at four depths: 1.25 cm, 2.5 cm, 7.5 cm, and 15 cm. Both soil moisture and temperature in-situ data were acquired simultaneously from the microwave radiometer measurements over a given field [20].

**Table 1.** Descriptions of the Beltsville Agricultural Research Center (BARC) test sites in the four-year experiment.

Year	Location	Texture	Sand (%)	Silt (%)	Clay (%)
1979	Elinsboro	Sandy loam	68	21	11
1980	Elinsboro	Sandy loam	68	21	11
1981	Edmonston	Sandy loam	67	18	15
	South Farm	Loam	31	44	25
1982	Edmonston	Sandy loam	68	21	11
	South Farm	Loam	34	42	24
	Gish	Loam/clay loam	24	47	29

### 3. Methodology

#### 3.1. Surface Emission Model

The surface emission model describes the relationship between the effective surface reflectivity and the Fresnel reflectivity through by parameterizing different effects from surface roughness. Considering that the non-coherent component is negligible at low frequencies, the  $H_p$  model was developed. This model has been widely used in various L-band radiometer algorithms [14]. However, the parameters of surface roughness in this model are empirically assigned according to different regions. These uncertain values introduce significant errors in heterogeneous surfaces. Recently, Chen [9] developed a simplified surface emission model according to the AIEM simulated database:

$$R_p = A_1 (s/l)^{B_1} r_p^{C_1} \quad (1)$$

$$R_q = A_2 (s/l)^{B_2} r_q^{C_2} \quad (2)$$

$$X(\theta, p) = e + f \times \theta + g \times \theta^2 + h \times \theta^3 \quad (3)$$

where  $R_p$  and  $R_q$  are the effective reflectivities;  $r_p$  and  $r_q$  are the Fresnel reflectivities;  $\theta$  is the incidence angle;  $s$  is the Root Mean Square (RMS) height;  $l$  is the correlation length; and the coefficients  $A$ ,  $B$ , and  $C$  are dependent only on the polarization and incidence angle, which can be acquired from Equation (3) using the AIEM simulated database in the previous study.

This model selects the ratio  $s/l$  as the surface roughness parameter based on the  $H_p$  model. The parameter  $C$  is used to correct the sensitivity of the surface emission to the soil moisture [9]. Although  $s$  and  $l$  cannot be measured easily from the surface, this form of the model unifies the surface roughness parameters in V- and H-polarization, which partially eliminates surface roughness effects through dual polarization. By cancelling out the surface roughness variable  $s/l$  from Equations (1) and (2), the relationship between the effective reflectivity and the Fresnel reflectivity can be simply derived easily:

$$\frac{R_p}{R_q^{B_2/B_1}} = \frac{A_1}{A_2^{B_2/B_1}} \times \frac{r_p^{C_1}}{r_q^{C_2 \cdot B_1/B_2}} \quad (4)$$

While there are only four parameters in this equation, it is not easy to solve in a direct way. The left side of Equation (4) includes the effective reflectivities  $R_p$  and  $R_q$ , which can be calculated from the dual-polarization brightness temperature. The Fresnel reflectivities  $r_p$  and  $r_q$  are the two unknown quantities that make this equation underdetermined.

In recent years, the relationship between the Fresnel reflectivities in dual polarization proved to be a power function, according to simulated data. Hong gave an approximate derivation through a Taylor series, which was verified by sensitivity studies and analytical derivation [24]:

$$r_p = r_q^A \quad (5)$$

$$A = 1/\cos^2\theta \quad (6)$$

The Hong approximation has been applied in various remote sensing applications [25–27]. In this study, Equation (4) can be simplified with this approximate relationship. By inserting Equations (5) and (6) into Equation (4),  $r_p$  can be replaced by  $r_q$ . Then, Equation (4) can be expressed as follows:

$$\frac{R_p}{R_q^{B_2/B_1}} = \frac{A_1}{A_2^{B_2/B_1}} \times r_q^{(A \cdot C_1 - \frac{C_2 \times B_1}{B_2})} \quad (7)$$

The seven coefficients can be combined into three new coefficients, providing a clear relationship between the dual-polarization effective reflectivity and the Fresnel reflectivities  $r_q$ :

$$\frac{R_p}{R_q^a} = b \times r_q^c \quad (8)$$

The relationships between the coefficients in Equations (7) and (8) are as follows:

$$a = B_1/B_2 \quad (9)$$

$$b = A_1 / \left( A_2^{B_1/B_2} \right) \quad (10)$$

$$c = A \times C_1 - (C_2 \times B_1) / B_2 \quad (11)$$

where  $a$ ,  $b$ , and  $c$  can be determined from regression analyses according to the AIEM simulated database.

### 3.2. Soil Moisture Retrieval Model

For bare surfaces, the radiation transfer equation can be simplified as follows:

$$T_{Bp} = (1 - R_p) T_e \quad (12)$$

$$T_{Bq} = (1 - R_q) T_e \quad (13)$$

where  $T_{Bp}$  and  $T_{Bq}$  are the dual polarization microwave brightness temperatures, and  $T_e$  is the effective surface temperature, which can be derived from semi-empirical models or replaced by surface temperature.

Combining Equations (12) and (13) into Equation (8), the Fresnel reflectivities  $r_q$  can be expressed as follows:

$$r_q = \left( \frac{(T_e - T_{Bp}) T_e^{a-1}}{b \times (T_e - T_{Bq})^a} \right)^{1/c} \quad (14)$$

Another form of the Fresnel reflectivity equation was proposed by Liou [28]. In this equation, the real part of the soil dielectric  $\epsilon$  is replaced by the adjusted real refractive index  $N_r$ . The adjusted real refractive index has a similar physical meaning as the soil dielectric, which also depends on soil properties. Therefore, this form of the Fresnel reflectivity equation can be applied to soil moisture retrieval. The complete form of equation is written as follows:

$$r_q = \left| \frac{\cos\theta - \sqrt{N_r^2 - \sin^2\theta}}{\cos\theta + \sqrt{N_r^2 - \sin^2\theta}} \right|^2 \quad (15)$$

$$N_r = \frac{\sqrt{2}}{2} \left\{ n_r^2 - n_i^2 + \sin^2\theta + \left[ (n_r^2 - n_i^2 - \sin^2\theta)^2 + 4n_r^2 n_i^2 \right]^{1/2} \right\}^{1/2} \quad (16)$$

where  $N_r$  is the adjusted real refractive index and the refractive index  $n = n_r - in_i$ . Here,  $n_i$  are the real and imaginary parts of the refractive index, respectively, which can be derived from the complex dielectric constant:

$$\begin{cases} \epsilon' = n_r^2 - n_i^2 \\ \epsilon'' = 2n_r n_i \end{cases} \quad (17)$$

$$\begin{cases} n_r = \sqrt{\frac{\sqrt{(\epsilon')^2 + (\epsilon'')^2} + \epsilon'}{2}} \\ n_i = \sqrt{\frac{\sqrt{(\epsilon')^2 + (\epsilon'')^2} - \epsilon'}{2}} \end{cases} \quad (18)$$

where  $\epsilon'$  and  $\epsilon''$  are the real and imaginary parts of the complex dielectric constant, respectively.

An analytic solution of Equation (15) for a non-absorbing material was given by Sohn [29]. In this study, a similar form of the solution will be extended to absorbing media.

By taking the square root of Equation (15),  $r_q^{1/2}$  can be written as follows:

$$r_q^{1/2} = \left| \frac{1 - N_r^2}{\left(\cos\theta + \sqrt{N_r^2 - \sin^2\theta}\right)^2} \right| \quad (19)$$

where  $N_r = \sin\theta_i/\sin\theta_t$ ,  $\theta_i$  is the incidence angle, and  $\theta_t$  is the refracted angle. According to the radiative transfer process, the wave penetrates through the air to the soil or water. Air is an optically thinner medium compared to soil and water. Based on Snell's law,  $N_r > 1$ . By removing the absolute value, the right side of Equation (19) can be simplified as follows:

$$r_q^{1/2} = \frac{N_r^2 - 1}{\left(\cos\theta + \sqrt{N_r^2 - \sin^2\theta}\right)^2} \quad (20)$$

After taking the square root of both sides of Equation (20), it can be rewritten in the following form:

$$\sqrt{N_r^2 - \sin^2\theta} = \frac{(N_r^2 - 1)^{1/2}}{r_q^{1/4}} - \cos\theta \quad (21)$$

Taking the squares of both sides of Equation (21) yields Equation (22):

$$N_r^2 - \sin^2\theta = \frac{(N_r^2 - 1)}{r_q^{1/2}} - 2\cos\theta \frac{(N_r^2 - 1)^{1/2}}{r_q^{1/4}} + \cos^2\theta \quad (22)$$

The same items can be merged as follows:

$$(N_r^2 - 1) \left( \frac{r_q^{1/2} - 1}{r_q^{1/2}} \right) = -2\cos\theta \frac{(N_r^2 - 1)^{1/2}}{r_q^{1/4}} \quad (23)$$

Taking the square of both sides of Equation (23) yields Equation (24):

$$(N_r^2 - 1)^2 \frac{(r_q^{1/2} - 1)^2}{r_q} = 4\cos^2\theta \frac{(N_r^2 - 1)}{r_q^{1/2}} \quad (24)$$

Arranging Equation (24) yields Equation (25):

$$(N_r^2 - 1) \left[ \frac{(r_q^{1/2} - 1)^2}{r_q} (N_r^2 - 1) - \frac{4\cos^2\theta}{r_q^{1/2}} \right] = 0 \quad (25)$$

The second term on the left side is zero because  $N_r > 1$ . Therefore, Equation (25) can be rewritten as follows:

$$\frac{(r_q^{1/2} - 1)^2}{r_q} (N_r^2 - 1) - \frac{4\cos^2\theta}{r_q^{1/2}} = 0 \quad (26)$$

After simplification, the adjusted real refractive index  $N_r$  can be expressed by:

$$N_r = \sqrt{1 + \frac{4r_q^{1/2} \cos^2\theta}{(r_q^{1/2} - 1)}} \tag{27}$$

In this study, a relationship between the adjusted real refractive index and soil moisture is proposed. The model form is similar to that of the Hallikainen dielectric constant model [30], which is as follows:

$$\epsilon' = (a_0 + a_1S + a_2C) + (b_0 + b_1S + b_2C) m_v + (c_0 + c_1S + c_2C) m_v^2 \tag{28}$$

where  $S$  and  $C$  are the percentage contents of sand and clay, respectively,  $\epsilon'$  is the real part of the complex dielectric constant, and  $m_v$  is the volumetric soil moisture.

The new soil moisture retrieval model is developed by substituting the left side of the Hallikainen model  $\epsilon'$  into the adjusted real refractive index  $N_r$ :

$$N_r = (a_0 + a_1S + a_2C) + (b_0 + b_1S + b_2C) m_v + (c_0 + c_1S + c_2C) m_v^2 \tag{29}$$

The coefficients of this model ( $a_0, a_1, a_2, b_0, b_1, b_2, c_0, c_1,$  and  $c_2$ ) can be determined through regression analyses according to the dielectric constant simulated database.

The quadratic equation with one unknown in Equation (29) has two solutions, one of which is soil moisture. The only auxiliary data required by this model are the percentage contents of sand and clay, which can be derived from field investigations. Soil moisture can then be calculated using the soil dielectric model through the one unknown quantity  $N_r$ . After simplification, the volumetric soil moisture can be expressed as follows. The integral scheme for this methodology is illustrated in Figure 1:

$$m_v = \frac{-(b_0 + b_1S + b_2C) + \sqrt{(b_0 + b_1S + b_2C)^2 - 4(c_0 + c_1S + c_2C)(a_0 + a_1S + a_2C - N_r)}}{2(c_0 + c_1S + c_2C)} \tag{30}$$

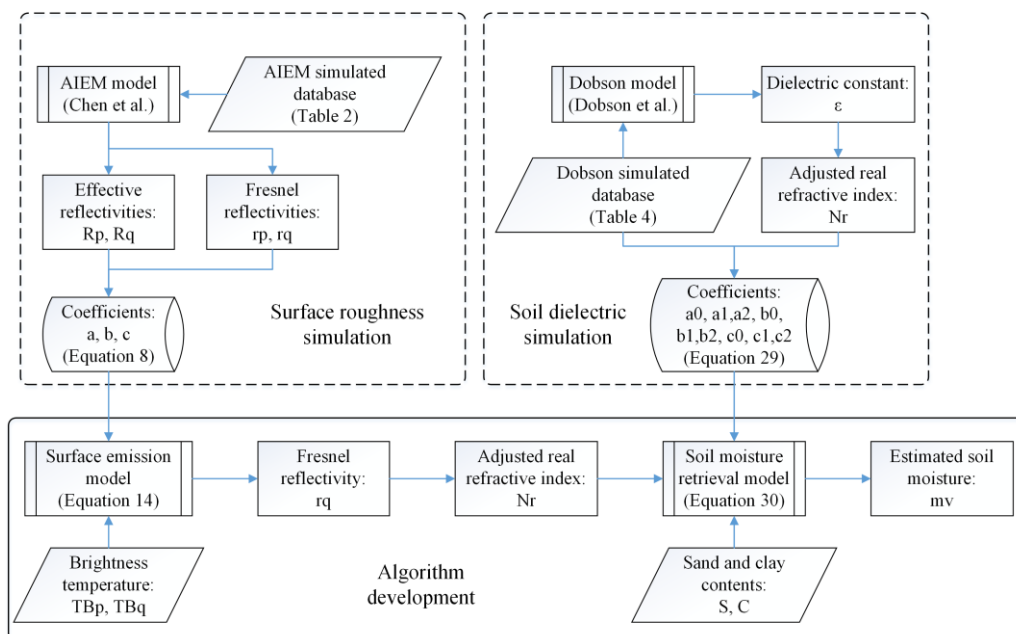


Figure 1. Scheme for methodology development of the novel simplified algorithm.

## 4. Results and Discussion

### 4.1. Soil Moisture Estimation with Simulated Data

To calibrate the coefficients of the surface emission model (Equation (8)), we generated a simulated surface emission database under the sensor parameters of the SMOS frequency, including 1.41 GHz and V- and H-polarization, using the AIEM model. This database covers a wide range of incidence angles, volumetric soil moisture, and roughness parameters, including RMS height, correlation length, and correlation functions. The detailed parameters used in the simulated database are summarized in Table 2.

**Table 2.** Surface roughness parameters and soil moisture used in the advanced integral equation model (AIEM) simulated database.

Soil Parameters	Minimum	Maximum	Interval
Soil moisture (%)	2	44	2
RMS <sup>1</sup> height (cm)	0.25	3	0.25
Correlation length (cm)	5	30	2.5
Incidence angle (degree)	5	60	5

<sup>1</sup> Root Mean Square (RMS).

The three coefficients ( $a$ ,  $b$ , and  $c$ ) at different incidence angles in Equation (8) are listed in Table 3. Figure 2 compares the Fresnel reflectivities  $r_q$  calculated using the AIEM model with those estimated using Equation (6) as a function of incidence angles from 5° to 60°. The root mean square errors (RMSEs) are lower at large incidence angles, especially at 45°. This tendency is caused by the simplified model style and a slope approximation for roughness. The parameter  $s/l$  used in Equations (1) and (2) better estimates surface roughness at large incidence angles, especially at 45°. At small angles, both H- and V-polarization have low accuracies. When the incidence angle is greater than 50°, H-polarization will introduce significant errors [9]. The simplified model was based on this hypothesis, resulting in similar values. In general, the error of the new surface emission model is smaller than 0.02 at all incidence angles, clearly indicating that this simplified emission model can replace the AIEM model over a wide range of surface conditions without significant errors.

**Table 3.** Coefficients of the surface emission model at different incidence angles.

Incidence Angle	$a$	$b$	$c$
5°	0.953487	1.00148	0.054886
10°	0.845617	1.004317	0.186599
15°	0.718362	1.005721	0.352128
20°	0.59251	1.003765	0.531698
25°	0.46837	0.997595	0.728534
30°	0.336077	0.987071	0.958948
35°	0.178412	0.972665	1.250999
40°	−0.032488	0.955735	1.650921
45°	−0.346537	0.939325	2.240814
50°	−0.872675	0.929568	3.189056
55°	−1.929771	0.938026	4.934479
60°	−4.929332	0.986903	9.172908

To verify the newly developed soil moisture retrieval model (Equation (30)), a dielectric constant simulated database was generated. Recent studies have shown that the five most common soil dielectric models have different superiorities in different conditions. The Dobson model exhibits good accuracy and has been used in many soil moisture retrieval algorithms [31,32]. Hence, the Dobson model was selected as the standard model in this study. The dielectric constant simulated database contained

more than 1.3 million groups of soil texture data, including a wide range of volumetric soil moisture, bulk density, soil temperature, and the percentage contents of sand and clay. The detailed parameters used in the simulated database are listed in Table 4. Then, this database was used to calibrate the coefficients of the soil moisture retrieval model in Equation (29). The results are listed in Table 5.

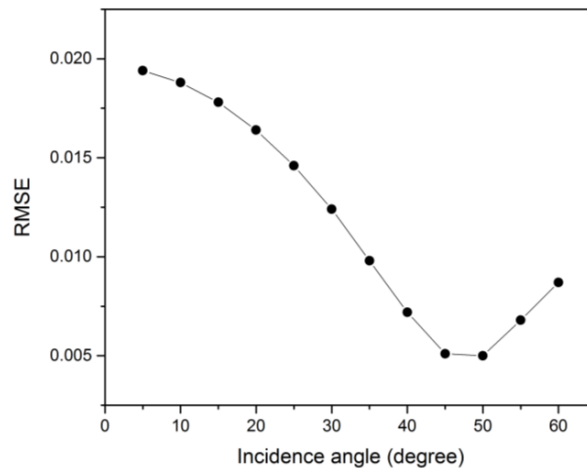


**Figure 2.** Comparison between the  $r_q$  estimated using the newly developed model and the Fresnel reflectivities  $r_q$  calculated using the advanced integral equation model (AIEM).

**Table 4.** Soil parameters used in the Dobson dielectric constant simulated database.

Soil Parameter	Minimum	Maximum	Interval
Soil moisture (%)	2	44	2
Bulk density (g/cm <sup>3</sup> )	0.9	1.7	0.1
Soil temperature (°C)	5	40	1
Sand content (%)	5	95	5
Clay content (%)	5	95	5

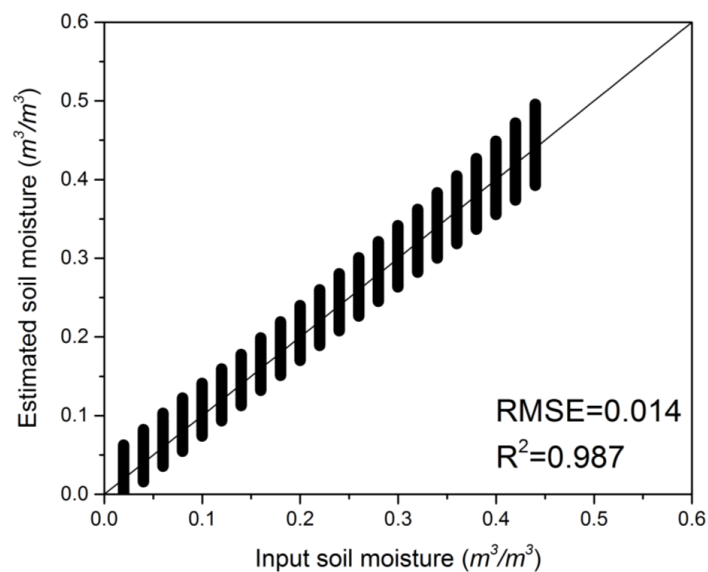
**Table 5.** Coefficients of the soil moisture retrieval model.

Coefficients	a0	a1	a2	b0	b1	b2	c0	c1	c2
Value	1.40	0.55	0.12	6.18	6.32	2.18	2.82	−9.80	−3.24

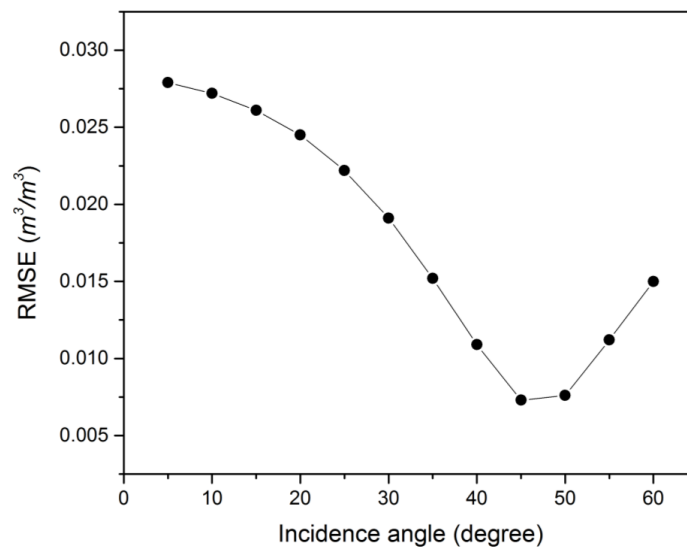
A comparison between the soil moisture estimated using the newly developed dielectric constant model and those input soil moisture calculated using the Dobson model is shown in Figure 3. The overall RMSE of the volumetric soil moisture is 0.014, suggesting a very good accuracy. The result indicates that the relationship between the adjusted real refractive index  $N_r$  and the volumetric soil moisture exhibits good agreement. The adjusted real refractive index  $N_r$  displays effects similar to the soil dielectric constant  $\epsilon$ . Both can reflect the dielectric properties of the soil. Therefore, the adjusted real refractive index can replace the soil dielectric properties in soil moisture retrieval. Only two soil parameter inputs and some empirical parameters are involved in the newly developed model, decreasing the workload and uncertainties associated with in situ measurements. The small deviation in soil moisture is due to simplification of the bulk density and soil temperature. In general, the model is simple and has a negligible error compared to the Dobson model simulations.

Figure 4 shows a comparison between the soil moisture estimated using the newly developed model and the input soil moisture calculated using the AIEM model. The overall RMSE is lower than 0.03 at all incidence angles from 5° to 60°. The accuracy of the newly developed model is better at large angles, exhibiting the same tendency as the previous surface emission model. These results clearly

indicate that the newly developed model has a high accuracy associated with soil moisture retrieval, without using surface roughness parameters.



**Figure 3.** Comparison between the soil moisture estimated using the newly developed soil moisture retrieval model and the input soil moisture calculated using the Dobson model.



**Figure 4.** Comparison of the soil moisture estimated using the newly developed model and the input soil moisture calculated using the AIEM model.

#### 4.2. Sensitivity Analysis

Considering the inevitable errors in measurements and models, a sensitivity analysis was conducted to evaluate the performance of this model. The input parameters were the microwave brightness temperatures and the surface temperatures from the AIEM simulated database. For the L-band radiometer, the radiometric uncertainty is 0.8 to 3 K for SMOS [1], while that of the newly launched SMAP is 1.3 K [2]. The maximum error of the Moderate Resolution Imaging Spectroradiometer (MODIS) in surface temperature retrieval is between 2 and 3 K [33]. Thus, different levels of Gaussian-distributed noise were randomly added to the simulated database in this study. The ranges of noise assigned to the brightness temperature and surface temperature span from 1 K to 5 K.

Figure 5 demonstrates the accuracy of the soil moisture retrieval model at different noise levels. The newly developed model responds differently to noise at different incidence angles. The large angles yield better results, exhibiting a similar trend as those shown in Figures 2 and 3. Figure 5a illustrates that low incidence angles, especially those at 5°, 10°, and 15°, exhibit poor performance when noise is introduced. Some of these values are over 10%, resulting in large uncertainty if the input data are of poor quality. Figure 5b shows that as the large incidence angles vary from 20° to 60°, almost all the RMSEs are under 5%. The most influential angle is 45°, which exhibits the lowest RMSE at every noise level. To satisfy the accuracy threshold of 0.04 m<sup>3</sup>/m<sup>3</sup>, which is the target of the SMOS and SMAP soil moisture products, the error of the measurement should be under 5 K, and the selected incidence angle should range from 35° to 60°.

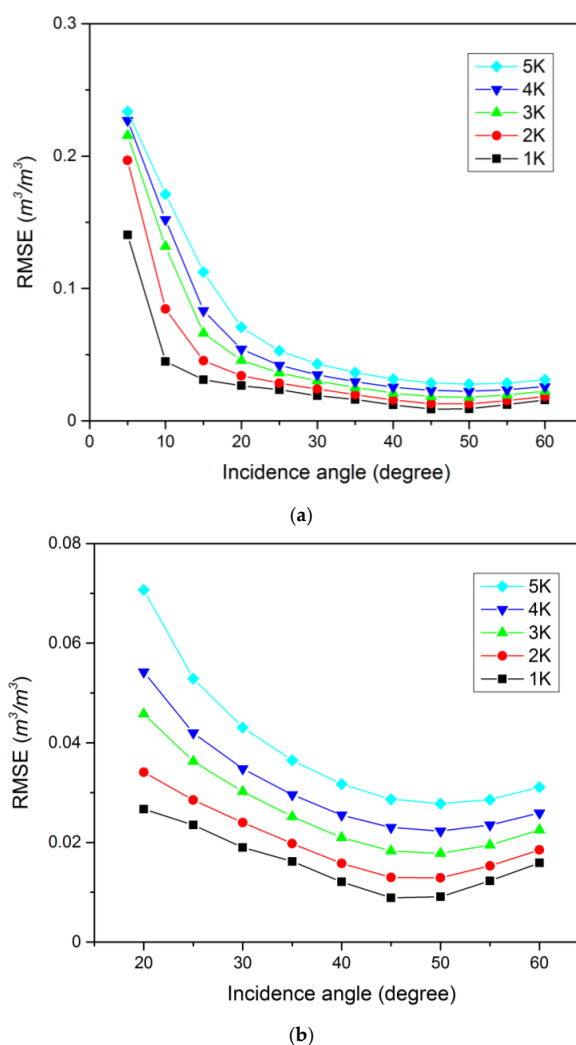


**Figure 5.** Responses of soil moisture retrieval root mean square errors (RMSEs) to errors in brightness temperature and surface temperature with incidence angles (a) from 5° to 60° and (b) from 20° to 60°.

#### 4.3. Soil Moisture Validation with *in Situ* Data

To further verify and test the soil moisture retrieval model developed in this study, the four-year experimental dataset from BARC from 1979 to 1982 was used, including both the V- and H-polarizations. Considering the inhomogeneous distribution of soil temperature and soil moisture in the vertical direction, the validation data are calibrated based on mean values. The soil temperature was selected based on the average values at depths of 0–2.5 cm and 2.5–5 cm, and soil moisture was obtained by averaging the soil moisture profile measurements from depths of 2.5 cm and 7.5 cm, which is in accordance with the corresponding penetration depths of L-band. Figure 6 compares

the volumetric soil moisture measurements with those estimated using the newly developed model. The RMSEs of volumetric soil moisture are 7.0%, 5.4%, 4.3%, and 3.4% at angles of 20°, 30°, 40°, and 50°, respectively. In particular, the accuracies at 40° and 50° fully satisfied the requirements of the SMOS and SMAP missions, indicating that the newly developed model is reliable and can effectively be applied for soil moisture retrieval.

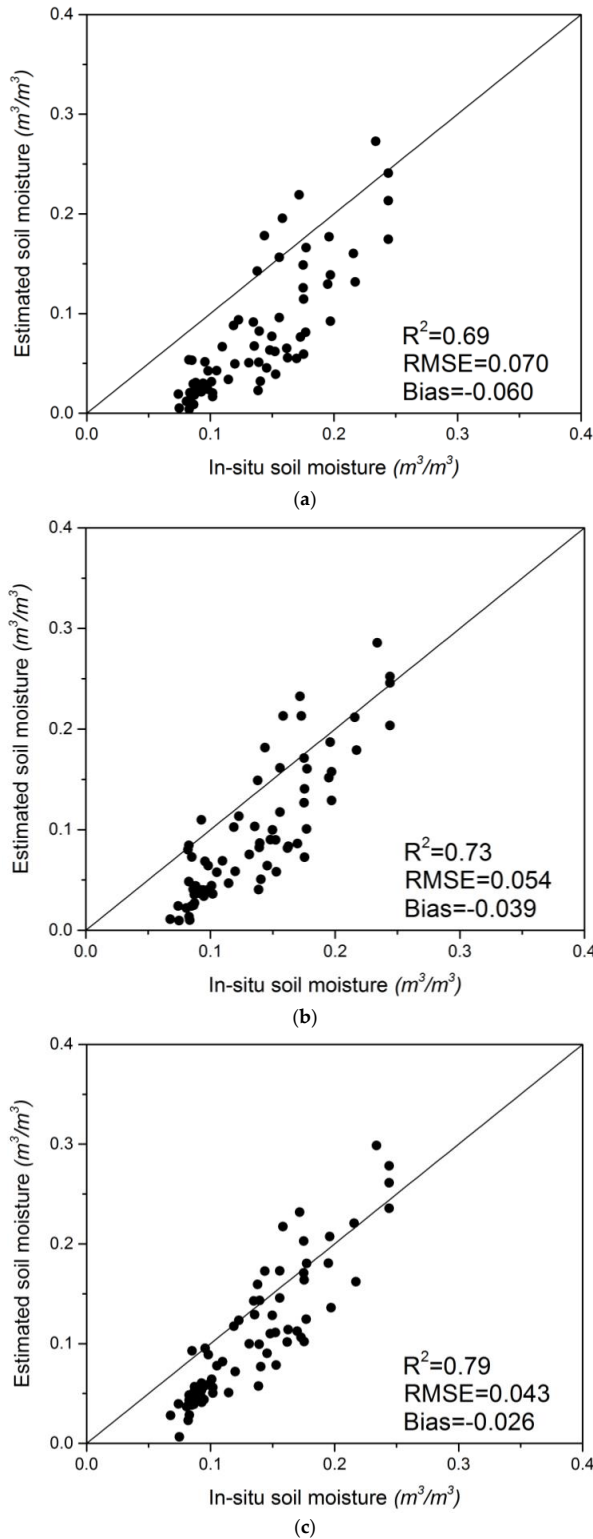
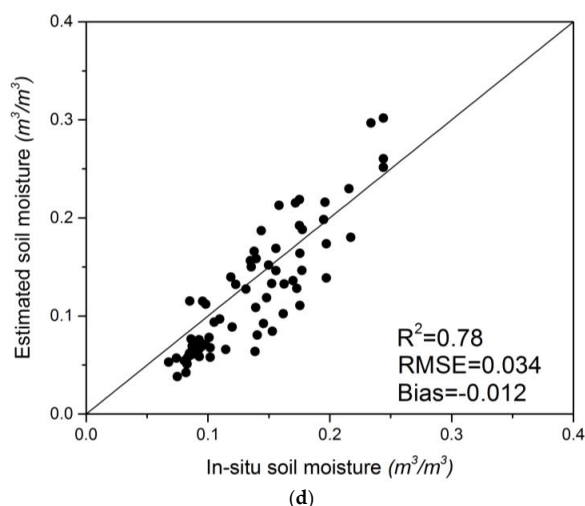


Figure 6. Cont.



**Figure 6.** Comparison of the soil moisture estimated using the newly developed model and the in situ soil moisture from the Beltsville Agricultural Research Center (BARC) from 1979 to 1982 at incidence angles of (a) 20°; (b) 30°; (c) 40°; and (d) 50°.

## 5. Conclusions

L-band radiometry shows great potential in soil moisture monitoring. Accurate modeling in L-band can significantly improve soil moisture retrieval. In this study, we developed a new algorithm for L-band soil moisture retrieval that combines two sub-algorithms. First, a new surface emission model was proposed to evaluate the effects of surface roughness. This model reduces the effects of surface roughness using dual-polarization surface reflectivity. The coefficients in this model were calibrated using the AIEM simulated database, which has been precisely proven over a wide range of surface conditions. The new method can be used directly without empirical parameters. Then, this model was applied for bare surface soil moisture retrieval using a soil moisture retrieval model. The retrieval model was calibrated using the Dobson simulated database based on the relationship between the adjusted real refractive index  $N_r$  and the volumetric soil moisture. The adjusted real refractive index  $N_r$ , which is physically deduced from the Fresnel reflectivity equation, shows a physical meaning similar to that of the soil dielectric  $\epsilon$ . In general, the algorithm proposed in this paper has many advantages compared with those of previous methods. This model utilizes an analytic solution method, which exhibits more stability and efficiency. The rigorous derivation was based on physical models, making the algorithm more reliable. The algorithm needs few ancillary soil data inputs, which makes it more applicable compared to previous methods. The only input parameters of the proposed algorithm are dual-polarization microwave brightness temperature, surface temperature, and the contents of sand and clay; it does not require any surface roughness parameters. In comparison with input soil moisture values simulated by the AIEM model, the soil moisture estimated using this model showed a very good accuracy, with RMSEs below 3% at all incidence angles. The proposed model performed well at higher incidence angles, particularly at 40°, 45°, and 50°. A sensitivity analysis showed that 45° is the best incidence angle for this model. The validation of the measured data were based on the four-year experiment conducted in Beltsville, Maryland. The results were particularly good for incidence angles of 20°, 30°, 40°, and 50°. The error was approximately 4% at incidence angles of 40° and 50°, which satisfies the requirements of the SMOS and SMAP mission. The results indicate that the model proposed in this paper shows excellent potential for soil moisture retrieval and that it is suitable for large incidence angle L-band radiometers such as SMAP. Although the overall accuracy was adequate, all the verified data were based on bare surface areas. Future studies will apply this new retrieval algorithm to vegetation coverage.

**Acknowledgments:** The work was supported by the Major State Basic Research Development Program of China “Spatial Scale Effects and Correction Models of Remote Sensing Information” under Grant No. 2013CB733402 and the National Nature Science Foundation of China under grant No. 41271379. The authors are indebted to the United States Department of Agriculture for providing the microwave and field data that were used in this manuscript.

**Author Contributions:** Bin Zhu conceived and designed the experiments with advice of Xiaoning Song and Xiaoguang Jiang. Bin Zhu performed the modeling and data analysis. Pei Leng supported the interpretation of the results. Chuan Sun and Ruixin Wang gave relevant technical support. All authors discussed the basic structure of the manuscript, and Bin Zhu finished the first draft. Xiaoning Song, Pei Leng and Xiaoguang Jiang reviewed and edited the draft. All authors read and approved the manuscript.

**Conflicts of Interest:** The authors declare no conflict of interest.

## References

1. Kerr, Y.H.; Waldteufel, P.; Wigneron, J.P.; Delwart, S.; Cabot, F.; Boutin, J.; Escorihuela, M.J.; Font, J.; Reul, N.; Gruhier, C.; et al. The SMOS mission: New tool for monitoring key elements of the global water cycle. *IEEE Proc.* **2010**, *98*, 666–687. [[CrossRef](#)]
2. Entekhabi, D.; Njoku, E.G.; O’Neill, P.E.; Kellogg, K.H.; Crow, W.T.; Edelstein, W.N.; Entin, J.K.; Goodman, S.D.; Jackson, T.J.; Johnson, J.; et al. The Soil Moisture Active Passive (SMAP) mission. *IEEE Proc.* **2010**, *98*, 704–716. [[CrossRef](#)]
3. Gharechelou, S.; Tateishi, R.; Sharma, R.C.; Johnson, B.A. Soil moisture mapping in an arid area using a land unit area (LUA) sampling approach and geostatistical interpolation techniques. *ISPRS Int. Geo-Inf.* **2016**. [[CrossRef](#)]
4. Le Vine, D.A.; Lagerloef, G.S.E.; Colomb, F.R.; Yueh, S.H.; Pellerano, F.A. Aquarius: An instrument to monitor sea surface salinity from space. *IEEE Trans. Geosci. Remote Sens.* **2007**, *45*, 2040–2050. [[CrossRef](#)]
5. Shi, J.C.; Dong, X.L.; Zhao, T.J.; Du, J.Y.; Jiang, L.M.; Du, Y.; Liu, H.; Wang, Z.Z.; Ji, D.B.; Xiong, C.; et al. Wcom: The science scenario and objectives of a global water cycle observation mission. In Proceedings of the 2014 IEEE International Geoscience and Remote Sensing Symposium, Quebec City, QC, Canada, 13–18 July 2014; IEEE: New York, NY, USA, 2014; pp. 3646–3649.
6. Chen, K.S.; Wu, T.D.; Tsang, L.; Li, Q.; Shi, J.C.; Fung, A.K. Emission of rough surfaces calculated by the integral equation method with comparison to three-dimensional moment method simulations. *IEEE Trans. Geosci. Remote Sens.* **2003**, *41*, 90–101. [[CrossRef](#)]
7. Choudhury, B.J.; Schmugge, T.J.; Chang, A.; Newton, R.W. Effect of surface-roughness on the microwave emission from soils. *J. Geophys. Res.-Oceans Atmos.* **1979**, *84*, 5699–5706. [[CrossRef](#)]
8. Shi, J.C.; Chen, K.S.; Li, Q.; Jackson, T.J.; O’Neill, P.E.; Tsang, L. A parameterized surface reflectivity model and estimation of bare-surface soil moisture with L-band radiometer. *IEEE Trans. Geosci. Remote Sens.* **2002**, *40*, 2674–2686.
9. Chen, L.; Shi, J.C.; Wigneron, J.P.; Chen, K.S. A parameterized surface emission model at L-band for soil moisture retrieval. *IEEE Geosci. Remote Sens. Lett.* **2010**, *7*, 127–130. [[CrossRef](#)]
10. Guo, P.; Shi, J.C.; Liu, Q.; Du, J.Y. A new algorithm for soil moisture retrieval with L-band radiometer. *IEEE J. Sel. Top. Appl. Earth Obs. Remote Sens.* **2013**, *6*, 1147–1155. [[CrossRef](#)]
11. Jia, Y.Y.; Tang, B.H.; Zhang, X.Y.; Li, Z.L. Estimation of land surface temperature and emissivity from AMSR-E data. In Proceedings of the IGARSS: 2007 IEEE International Geoscience and Remote Sensing Symposium, Vols 1–12: Sensing and Understanding Our Planet, Barcelona, Spain, 23–28 July 2007; IEEE: New York, NY, USA, 2007; pp. 1849–1852.
12. Liu, Z.L.; Wu, H.; Tang, B.H.; Qiu, S.; Li, Z.L. An empirical relationship of bare soil microwave emissions between vertical and horizontal polarization at 10.65 GHz. *IEEE Geosci. Remote Sens. Lett.* **2014**, *11*, 1479–1483.
13. Jackson, T.J. Measuring surface soil-moisture using passive microwave remote-sensing. *Hydrol. Process.* **1993**, *7*, 139–152. [[CrossRef](#)]
14. Wigneron, J.P.; Kerr, Y.; Waldteufel, P.; Saleh, K.; Escorihuela, M.J.; Richaume, P.; Ferrazzoli, P.; de Rosnay, P.; Gurney, R.; Calvet, J.C.; et al. L-band microwave emission of the biosphere (L-MEB) model: Description and calibration against experimental data sets over crop fields. *Remote Sens. Environ.* **2007**, *107*, 639–655. [[CrossRef](#)]

15. O'Neill, P.E. Microwave remote-sensing of soil-moisture—A comparison of results from different truck and aircraft platforms. *Int. J. Remote Sens.* **1985**, *6*, 1125–1134. [[CrossRef](#)]
16. Wang, J.R. Effect of vegetation on soil-moisture sensing observed from orbiting microwave radiometers. *Remote Sens. Environ.* **1985**, *17*, 141–151. [[CrossRef](#)]
17. Schmugge, T.; O'Neill, P.E.; Wang, J.R. Passive microwave soil-moisture research. *IEEE Trans. Geosci. Remote Sens.* **1986**, *24*, 12–22. [[CrossRef](#)]
18. Al-Yaari, A.; Wigneron, J.P.; Kerr, Y.; de Jeu, R.; Rodriguez-Fernandez, N.; van der Schalie, R.; Al Bitar, A.; Mialon, A.; Richaume, P.; Dolman, A.; et al. Testing regression equations to derive long-term global soil moisture datasets from passive microwave observations. *Remote Sens. Environ.* **2016**, *180*, 453–464. [[CrossRef](#)]
19. Shi, J.C.; Du, Y.; Du, J.Y.; Jiang, L.M.; Chai, L.N.; Mao, K.B.; Xu, P.; Ni, W.J.; Xiong, C.; Liu, Q.; et al. Progresses on microwave remote sensing of land surface parameters. *Sci. China-Earth Sci.* **2012**, *55*, 1052–1078. [[CrossRef](#)]
20. Wang, J.; Shiue, J.; Engman, E.; McMurtrey, J.; Lawless, I.P.; Schmugge, T.J.; Jackson, T.J.; Gould, W.; Fuchs, J.; Calhoun, C.; et al. *Remote Measurements of Soil Moisture by Microwave Radiometers at BARC Test Site*; NASA, NASA Tech. Memo: Greenbelt, MD, USA, 1980.
21. Wang, J.; O'Neill, P.; Engman, E.; McMurtrey, J.; Lawless, I.P.; Schmugge, T.J.; Jackson, T.J.; Gould, W.; Fuchs, J.; Glazer, W. *Remote Measurements of Soil Moisture by Microwave Radiometers at BARC Test Site II*; NASA, NASA Tech. Memo: Greenbelt, MD, USA, 1982.
22. Wang, J.; Jackson, T.J.; Engman, E.; Gould, W.; Fuchs, J.; Glazer, W.; O'Neill, P.; Schmugge, T.J.; McMurtrey, J. *Microwave Radiometer Experiment of Soil Moisture Sensing at BARC Test Site Curing Summer 1981*; NASA, NASA Tech. Memo: Greenbelt, MD, USA, 1984.
23. O'Neill, P.; Jackson, T.J.; Blanchard, B.; van den Hoek, R.; Gould, W.; Wang, J.; Glazer, W.; McMurtrey, J. *Soil Hydraulic Properties on Passive Microwave Sensing of Soil Moisture: Data Report for the 1982 Field Experiments*; NASA, NASA Tech. Memo: Greenbelt, MD, USA, 1983.
24. Hong, S. Retrieval of refractive index over specular surfaces for remote sensing applications. *J. Appl. Remote Sens.* **2009**, *3*, 033560. [[CrossRef](#)]
25. Hong, S. Detection of small-scale roughness and refractive index of sea ice in passive satellite microwave remote sensing. *Remote Sens. Environ.* **2010**, *114*, 1136–1140. [[CrossRef](#)]
26. Hong, S. Global retrieval of small-scale roughness over land surfaces at microwave frequency. *J. Hydrol.* **2010**, *389*, 121–126. [[CrossRef](#)]
27. Hong, S. Surface roughness and polarization ratio in microwave remote sensing. *Int. J. Remote Sens.* **2010**, *31*, 2709–2716. [[CrossRef](#)]
28. Liou, K.N. *An Introduction to Atmospheric Radiation*, 2nd ed.; Academic Press: New York, NY, USA, 2002.
29. Sohn, B.J.; Lee, S.M. Analytical relationship between polarized reflectivities on the specular surface. *Int. J. Remote Sens.* **2013**, *34*, 2368–2374. [[CrossRef](#)]
30. Hallikainen, M.T.; Ulaby, F.T.; Dobson, M.C.; Elrayes, M.A.; Wu, L.K. Microwave dielectric behavior of wet soil. 1. Empirical-models and experimental-observations. *IEEE Trans. Geosci. Remote Sens.* **1985**, *23*, 25–34. [[CrossRef](#)]
31. Njoku, E.G.; Chan, S.K. Vegetation and surface roughness effects on AMSR-E land observations. *Remote Sens. Environ.* **2006**, *100*, 190–199. [[CrossRef](#)]
32. Jones, M.O.; Jones, L.A.; Kimball, J.S.; McDonald, K.C. Satellite passive microwave remote sensing for monitoring global land surface phenology. *Remote Sens. Environ.* **2011**, *115*, 1102–1114. [[CrossRef](#)]
33. Justice, C.O.; Vermote, E.; Townshend, J.R.G.; Defries, R.; Roy, D.P.; Hall, D.K.; Salomonson, V.V.; Privette, J.L.; Riggs, G.; Strahler, A.; et al. The moderate resolution imaging spectroradiometer (MODIS): Land remote sensing for global change research. *IEEE Trans. Geosci. Remote Sens.* **1998**, *36*, 1228–1249. [[CrossRef](#)]

